Outer Membrane Vesicles from bacteria expressing the HlyF/CprA family of enzymes are more efficient at delivering their cargo into host cells.

Frédéric Taieb[a#*], Laure David[a#], Camille Pin[a], Audrey Goman[a], Asja Garling[a], Christelle Marrauld[a], Marine Colson[a], Marie Pénary[a], and Eric Oswald[a,b*]

[a]Institut de Recherche en Santé Digestive (IRSD), Université de Toulouse, INSERM, INRAE, ENVT, UPS, Toulouse, France; [b]Service de Bactériologie-Hygiène, Centre Hospitalier Universitaire de Toulouse, Hôpital Purpan, France

# These authors contributed equally

*Address correspondence to: eric.oswald@inserm.fr; frederic.taieb@inrae.fr

Keywords: Outer Membrane Vesicle, HlyF, CprA, *Escherichia coli, Pseudomonas aeruginosa*

Abbreviations:

AUC: area under the curve

CtxB: cholera toxin B

E. coli: *Escherichia coli*

FRET: fluorescence resonance energy transfer

HBSS: Hanks' balanced salt solution

HlyF: hemolysin F

LPS: lipopolysaccharide

mut: mutated

M/PAMPs: microbial/pathogen-associated molecular patterns

NMEC: neonatal meningitis associated *E. coli*

OMP(s): outer membrane protein(s)

OMV(s): outer membrane vesicle(s)

P. aeruginosa: *Pseudomonas aeruginosa*

SDR: short chain dehydrogenase/reductase

TEM: transmission electron microscopy

UPEC: uropathogenic *E. coli*

wt: wild-type

Abstract

HlyF, a cytoplasmic short-chain dehydrogenase/reductase enzyme encoded by a virulence plasmid in *Escherichia coli*, and its ortholog CprA, encoded notably by the chromosome of *Pseudomonas aeruginosa*, drive the production of specific outer membrane vesicles (OMVs). These OMVs have been shown to have the unique abilities to disrupt autophagic flux and exacerbate inflammatory response in host cells. In this study, we demonstrate that these OMVs have improved cargo delivery efficiency through a clathrin-independent internalization pathway into host cells, by directly fusing with the plasma membrane of the host cell. These results reveal an uncovered role of the HlyF/CprA enzyme family in enhancing OMV function through a unique internalization pathway and unveil a novel mechanism driving OMV-mediated virulence.

Introduction

Gram-negative bacteria, as all cells, release extracellular vesicles (EVs). Among various subtypes, EVs that bud from their outer membrane are called outer membrane vesicles (OMVs). These nanoparticles convey a variety of molecular components originating from both the outer membrane and the periplasm of the parent bacteria. These molecules include lipids, lipopolysaccharides (LPS), outer membrane proteins (OMPs) and periplasmic compounds including toxins [1-3]. By exposing surface pro-inflammatory antigens and microbial/pathogen-associated molecular patterns (M/PAMPs), OMVs modulate both innate and acquired immune responses, potentially triggering lethal sepsis in animal models [4, 5]. Many studies have demonstrated that eukaryotic cells can internalize bacterial vesicles by endocytosis, meaning that OMVs deliver into host cells not only membrane components including lipids, OMPs, PAMPs, and LPS but also toxins and various periplasmic molecules, thus participating in the host-pathogen interaction [6, 7]. Therefore, OMVs are now recognized to play pivotal roles in various biological processes, particularly in the context of virulence.

We previously characterized HlyF in *Escherichia coli* and CprA in *Pseudomonas aeruginosa* as strictly cytoplasmic enzymes that induce the production of specialized OMVs able of block the autophagic flux in intoxicated eukaryotic cells [8, 9]. As autophagy contributes to the negative

feedback loop of inflammasome activation, this OMV-dependent inhibition of autophagy results in the exacerbation of the non-canonical inflammatory response triggered by OMV-mediated PAMPs delivery, eventually leading to cell death [8-10]. The expression of HlyF and CprA has been further linked to pathogenicity of *E. coli* and *P. aeruginosa* in avian colibacillosis [11] and murine models of sepsis [9] or urosepsis [12]. In this study, we demonstrate that OMVs produced by HlyF/CprA expressing bacteria have improved cargo delivery efficiency into host cells. Our results revealed that HlyF/CprA induces enhanced entry of OMVs into the host cell via a clathrin-independent endocytic pathway by promoting their direct fusion with the host plasma membrane, stimulating the delivery of their virulence factors into host cells to promote bacterial pathogenicity.

Results

Expression of HlyF does not affect the loading of TEM-1 ß-lactamase into OMVs.

To investigate the kinetic of vesicle uptake into eukaryotic cells, we monitored the delivery of the β-lactamase cargo loaded into OMV. In Gram-negative bacteria, the β-lactamase is naturally translocated into the periplasmic space by the sec-system pathway where it acquires its active form following the cleavage of the N-terminal signal peptide and oxidative folding [13]. Thus, OMVs, which are filled with periplasmic contents, embark β-lactamase as cargo (figure 1A). We purified OMVs loaded with ß-lactamase from *E. coli* co-transformed with plasmids encoding either wild-type HlyF ($HlyF^{wt}$) or an inactive HlyF mutated in the SDR catalytic site ($HlyF^{mut}$), together with the high-copy pUC19 plasmid expressing TEM-1 β-lactamase. Western blot quantification of TEM-1 β-lactamase in both OMV types, using the outer membrane protein A (OMPA) as a loading control, revealed comparable protein levels, indicating that HlyF does not affect vesicle's enzyme incorporation (figure 1B). Enzymatic activity was then determined by measuring the absorbance of hydrolyzed chromogenic substrate nitrocefin over time in presence of purified OMVs. Both the reaction slope and the total enzymatic activity showed that OMVs from *E. coli* expressing either wild-type or mutant HlyF, which contain equivalent amounts of TEM-1 as confirmed by western blot analysis, exhibit comparable β-lactamase activity (figure 1C and supplementary figure 1A). Microscopic observation revealed a consistent similar vesicle structure, as expected for OMV formation, along with similar apparent diameter sizes for both $HlyF^{wt}$ and $HlyF^{mut}$ OMVs (supplementary figure 1B). Subsequent assessment of OMV size distribution via dynamic light scattering (DLS)

yielded comparable results for both HlyF^{wt} and HlyF^{mut} OMVs, with a mean diameter falling within the range of 21-24 nm (supplementary figure 1C). Coomassie blue and silver staining of gel electrophoresis revealed identical protein profile for both type of OMVs (supplementary figure 1D). Together, these analyses showed that OMVs produced by bacteria expressing active or non-active HlyF exhibit similar protein composition, including TEM-1 ß-lactamase and OmpA, as well as comparable structural and biophysical features.

OMVs produced by HlyF-expressing bacteria accumulate their cargo within host cells more efficiently than control OMVs.

To investigate the kinetic of cargo delivery into eukaryotic cells, we used a reporter system based on detection of β-lactamase activity, using the fluorescence resonance energy transfer (FRET) substrate CCF4-AM. This substrate consists of a cephalosporin core linking 7-hydroxycoumarin to fluorescein (LiveBLAzer^{TM}). Enzymatic cleavage of the ß-lactam ring of cephalosporin disrupts CCF4 FRET, resulting in a fluorescence shift from green to blue enabling quantification of β-lactamase cargo delivery by OMV (figure 2 A). Purified OMVs containing a normalized quantity of β-lactamase were added to HeLa cells preloaded with CCF4. Monitoring the ratio of blue/green fluorescence using microplate spectrophotometer enables precise quantification of β-lactamase TEM-1 released into host cells over time (figure 2B). The total enzyme delivery was evaluated by calculating the area under the curves (AUC). AUC analysis revealed that addition of OMVs results in effective delivery of ß-lactamase. However, HlyF^{wt} OMVs resulted in a greater accumulation of ß-lactamase into HeLa cells compared to HlyF^{mut} OMVs (figure 2C). As shown in figure 2D, the steeper slope of the blue/green fluorescence curve for HlyF^{wt} OMVs suggests that an accelerated rate of accumulation of the enzyme accounts for their greater overall delivery compared to HlyF^{mut} OMVs. To exclude the contribution of free β-lactamase released from OMVs to the FRET disruption of CCF4 and increased AUC, the experiment was repeated with pronase-treated OMVs. OMVs protected ß-lactamase cargo from protease digestion as AUC level is preserved in pronase-treated samples regardless the type of OMVs (supplementary figure 2). In addition to demonstrating that AUC level is essentially dependent on OMVs-associated ß-lactamase cargo, these results suggest that the delivery mechanism of OMVs is independent of proteins exposed on the OMV surface. Since the experiments were performed in HeLa cells, which display a transformed metabolic profile, we sought to verify that our observations also apply using primary cells—specifically,

mouse bone marrow-derived macrophages (BMDMs). Accordingly, we validated the HlyFwt OMV-induced increase of ß-lactamase activity in CCF4-loaded BMDM (figure 2D), confirming this effect in a more physiologically relevant context.

The enhanced delivery of OMV cargo into host cells by OMVs from HlyF-expressing bacteria is not due to the inhibition of autophagy.

Given that HlyF^{wt} OMVs have been shown to block autophagosome-lysosome fusion [8, 10], it can be hypothesized that degradation of OMVs internalized following endocytosis into endosome and potential fusion with lysosome is also disrupted [3, 14, 15]. This inhibition could lead to the stabilization of OMV's cargo, including TEM-1 β-lactamase, increasing CCF4-AM cleavage and thus increasing the associated AUC. To investigate this hypothesis, we used autophagy inhibitors, chloroquine and bafilomycin [16]. If the increased AUC were due to TEM stabilization induced by HlyF^{wt} OMVs as a result of autophagic blockage [8], then, autophagic inhibitors would be expected to boost AUC in HlyF^{mut} OMV-treated cells to the same level as that observed with HlyF^{wt} OMVs. As shown in figure 3A and 3B, the addition of these pharmacological inhibitors did not lead to an increase in AUC, suggesting that the rise in ß-lactamase activity is unrelated to autophagic dysfunction but rather results from improved cargo delivery by OMVs from bacteria expressing HlyF.

OMVs from bacteria producing HlyF^{wt} enter into cell by a clathrin-independent pathway

OMVs derived from *E. coli* have been reported to enter host cells through both clathrin- and caveolin-dependent endocytosis pathways [3, 14, 17–21]. The formation of these vesicles requires multiple proteins that promote plasma membrane invagination and vesicle scission, a process mediated by the GTPase dynamin, which pinches off the vesicle to generate early endosomes [22, 23]. To further investigate the HlyF-dependent mechanism of OMV internalization, we used Dynasore, a dynamin GTPase inhibitor that blocks both clathrin- and caveolin-mediated endocytosis [24–26]. CCF4-loaded cells were treated or not with Dynasore and exposed to either HlyF^{wt} or HlyF^{mut} OMVs containing equivalent amounts of TEM-1 cargo. Consistent with previous observations for OMVs produced by *E. coli* strains lacking *hlyF* [3, 14, 17–20], Dynasore inhibited the entry of OMVs from bacteria expressing the inactive HlyF variant. Remarkably, although Dynasore treatment reduced the area under the curve (AUC) compared with untreated controls, a substantial fraction of HlyF^{wt} OMV internalization

persisted in inhibitor-treated cells (figure 3C). The partial β-lactamase activity detected in the presence of Dynasore may thus reflect the higher intrinsic uptake efficiency of HlyF^{wt} OMVs. To exclude the possibility that this effect resulted solely from their increased baseline activity, we repeated the assay using 2.5-fold fewer HlyF^{wt} OMVs, adjusted to yield comparable AUC values between HlyF^{wt} and HlyF^{mut} OMVs in untreated cells. Under these conditions, Dynasore inhibited HlyF^{mut} OMV entry by nearly 80%, whereas internalization of HlyF^{wt} OMVs was reduced by only ~10% (Figure 3D). These findings indicate that HlyF confers upon OMVs the capacity to enter host cells through a dynamin-independent pathway. Notably, the observation that higher concentrations of HlyF^{wt} OMVs exhibited partial inhibition (~50%, Figure 3C), while lower concentrations were minimally affected (~10%, Figure 3D), suggests that at elevated OMV levels, uptake may rely in part on dynamin-dependent endocytosis once the alternative HlyF-mediated pathway becomes saturated.

HlyF promotes OMV internalization by direct fusion to host cell plasma membrane

To investigate the mechanism of HlyFwt OMV internalization in eukaryotic cells, we labeled OMV membranes with the lipophilic dye DiI, which spontaneously integrates into lipid bilayers. We first confirmed that HlyFmut and HlyFwt OMVs incorporated DiI with comparable efficiency (Supplementary figure 3) before exposing HeLa cells to the labeled vesicles. Cells treated with HlyFmut OMVs displayed punctate intracellular fluorescence, indicating that the dye remained confined within intact, internalized vesicles rather than diffusing into host membranes. In contrast, cells exposed to HlyFwt OMVs exhibited a faint and diffuse fluorescence pattern, nearly indistinguishable from background, consistent with dye redistribution into host plasma membranes (figure 4A). We next validated this finding using fluorescent liposomes generated from lipids extracted from BL21(DE3) strains expressing either HlyF^{mut} or HlyF^{wt} [9]. Upon incubation with HeLa cells, HlyF^{wt}-derived liposomes produced a diffuse fluorescence throughout the cell, whereas HlyF^{mut}-derived liposomes showed a punctate staining pattern (figure 4B). Together, these observations support a model in which HlyF^{mut} OMVs or liposomes enter cells via endocytosis and remain compartmentalized within endosomes, whereas HlyF^{wt} derived vesicles bypass endocytic trafficking by directly fusing with the plasma membrane. To further corroborate this hypothesis, we examined the involvement of plasma membrane lipid raft microdomains, previously shown to mediate *P. aeruginosa* OMV fusion [27]. We used FITC-labeled cholera toxin B subunit (CtxB–FITC), a well-

established lipid raft marker [28]. In untreated cells and those exposed to HlyF^{mut} OMVs, CtxB–FITC fluorescence appeared as distinct clusters, visible as green puncta corresponding to lipid raft domains. In contrast, cells treated with HlyF^{wt} OMVs displayed fewer and more diffusely distributed CtxB–FITC clusters (figure 4C), indicating a disruption of raft organization. Since dispersion of CtxB–FITC foci reflects alterations in membrane lipid dynamics [28], these findings suggest that, unlike HlyF^{mut} OMVs, which enter cells via endocytosis without affecting lipid organization, HlyF^{wt} OMVs fuse directly with the plasma membrane, thereby inducing lipid reorganization.

OMVs from clinical isolates of pathogenic E. coli *and* P. aeruginosa *strains expressing HlyF and CprA respectively, show enhanced cargo accumulation into host cells*

We next confirmed these results using clinical isolates of *E. coli* naturally expressing HlyF. OMVs were purified from the SP15 strain, a neonatal meningitis-causing *E. coli* (NMEC) [17], expressing either HlyF^{wt} or the inactive form of HlyF^{mut} [8] and from an uropathogenic *E. coli* (UPEC) strain, ECC166 wild-type and its isogenic *hlyF*-deleted strains [12]. We extended our investigation using OMVs from *P. aeruginosa* PAK strain expressing HlyF ortholog, CprA and the isogenic deleted strains [9]. All strains were transformed with TEM-1 ß-lactamase expressing plasmids (see material & method) and OMV concentration were normalized for equivalent enzyme load before addition on HeLa cells loaded with CCF4. Consistent with the results obtained with OMVs from BL21(DE3), OMVs produced by strains expressing active HlyF/CprA displayed higher AUC values than their corresponding hlyF/cprA-mutant strains, indicating that HlyF^{wt}/CprA OMVs mediated a more substantial delivery of TEM-1 β-lactamase in host cells compared with HlyF^{mut} OMVs or OMVs produced in absence of HlyF/CprA (figure 5A, B and C). Since all experiments utilized pairs of OMVs standardized for equivalent β-lactamase content, these findings demonstrate that OMVs derived from pathogenic HlyF/CprA-expressing bacteria promote cargo accumulation into host cells.

Discussion

We demonstrate that the HlyF/CprA enzymes promote the production of a distinct class of OMVs that deliver their cargo to host cells more efficiently and rapidly than OMVs from *hlyF*-negative strains. These results provide compelling evidence that the enzymatic activity of HlyF/CprA not only regulates OMV biogenesis but also determines their interaction mode with

eukaryotic membranes, potentially contributing to their specific property, i.e. blocking the autophagy flux. Using our β-lactamase reporter system combined with pharmacological inhibitors, we found that, unlike classical OMVs that use the clathrin- and dynamin-dependent endocytic pathway, HlyF^{wt} OMVs are internalized even in the presence of the dynamin inhibitor Dynasore. This reveals a previously unrecognized, dynamin-independent uptake mechanism. To our knowledge, this is the first report of such a pathway for *E. coli* OMVs, expanding the current paradigm of vesicle entry mechanisms.

Microscopic analyses provided additional insight into this distinctive uptake route. Whereas HlyF^{mut} OMVs generated punctate intracellular fluorescence consistent with endocytic uptake and vesicle integrity, HlyF^{wt} OMVs produced diffuse membrane-associated fluorescence, suggesting direct fusion of the vesicle bilayer with the host plasma membrane. Notably, vesicle reconstitution using liposomes generated with lipids from either wild-type or mutant HlyF strains recapitulated these distinct patterns, indicating that HlyF-modified lipids are the primary driver of this alternative entry mechanism. Lipid raft analysis using FITC-labeled cholera toxin B subunit (CtxB–FITC) further supported this hypothesis. In untreated cells and those exposed to HlyF^{mut} OMVs, CtxB–FITC fluorescence appeared as discrete clusters corresponding to stable raft microdomains. By contrast, HlyF^{wt} OMVs disrupted these clusters, dispersing the signal across the plasma membrane. Because raft clustering depends on lipid phase separation and membrane order, its loss is a hallmark of lipid mixing during fusion. These results strongly support that HlyF^{wt} OMVs enter host cells via direct fusion with the plasma membrane rather than classical endocytosis.

Fusion-mediated internalization provides a mechanistic explanation for the rapid and extensive cargo delivery observed with HlyF^{wt} OMVs. Unlike endocytosis, which requires vesicular trafficking and endosome maturation, direct fusion allows immediate and massive cytoplasmic release of OMV vesicular contents. This observation aligns with findings in *P. aeruginosa* harboring *cprA*, the HlyF ortholog, where OMVs also enter host cells through a dynamin-independent fusion mechanism [27].

Both bacterial and eukaryotic membranes consist of lipid bilayers whose composition controls physical properties, such as curvature, rigidity and phase miscibility, governing their fusogenic potential. Recent study suggest that HlyF/CprA enzymes are SDRs functioning as fatty acyl-CoA reductases (FARs) that could generate long-chain fatty alcohols incorporated into OMV lipids [10]. Although the exact lipid species remain unidentified, these enzymatic modifications likely

alter bilayer flexibility, decreasing membrane stability and lowering the energy barrier for fusion with host membranes. By reprogramming OMV lipid composition, HlyF/CprA may thus endow vesicles with enhanced ability to merge with lipid raft microdomains of the host plasma membrane, consistent with the observed alteration of CtxB staining. Furthermore, since lysosomes incorporates plasma membrane–derived components (PMID: 19672277), our findings suggest that OMV fusion may introduce HlyF-modified lipids into lysosomes, potentially compromising their integrity/function and thereby contributing to the HlyF-dependent inhibition of autophagic flux.

This mechanism extends beyond membrane biophysics and has major implications for bacterial virulence. Clinical *E. coli* and *P. aeruginosa* strains expressing HlyF/CprA produce OMVs with enhanced delivery capacity for a variety of virulence factors, including Shiga toxin (Stx), cytolethal distending toxin (CDT), and the CFTR inhibitory factor (Cif) [3, 8, 27, 33]. Direct OMV–plasma membrane fusion would enable these effectors to bypass endosomal sorting, resulting in their immediate release into the cytosol and direct interaction with intracellular targets. Furthermore, HlyF/CprA OMVs have been shown to impair autophagy by inhibiting autophagosome–lysosome fusion [11, 12]. This blockade prevents the degradation of internalized toxins and pathogen-associated molecular patterns (PAMPs), likely stabilizing their activity inside host cells. The combined effects of enhanced entry and impaired clearance may substantially exacerbate bacterial cytotoxicity and inflammation, consistent with *in vivo* data demonstrating worsened outcomes of infections caused by *hlyF/cprA*-positive strains [8–10].

The identification of *hlyF/cprA* homologs in other pathogenic species, including *Yersinia pestis* and *Ralstonia solanacearum* [10] underscores the evolutionary conservation and potential ubiquity of this strategy among Gram-negative bacteria. The widespread distribution of these enzymes suggests that lipid remodeling to modulate OMV–host interactions represents a common, yet underexplored, virulence mechanism. By tuning vesicle lipid composition, pathogens may control not only OMV production but also the efficiency, timing, and specificity of host cell intoxication. This concept expands the current understanding of OMV-mediated communication, highlighting that not only the vesicle cargo but also the mechanism of entry plays a key role in determining their function.

In conclusion, our findings identify HlyF/CprA as pivotal enzymes that remodel OMV lipid composition, conferring fusogenic properties that enable a novel, dynamin-independent mode of host cell entry. This fusion-based mechanism provides a rapid and efficient pathway

for bacterial cargo delivery and likely contributes to the heightened virulence of *hlyF/cprA*-positive pathogens. By linking lipid enzymology to vesicle–host membrane interactions, our study uncovers a fundamental aspect of OMV biology with broad implications for infection, immunity, and vesicle-based therapeutics. Future work should focus on defining the specific lipid species generated by HlyF/CprA and elucidating how these modifications modulate membrane phase behavior and fusion energetics. Such insights will not only deepen our understanding of bacterial pathogenesis but may also reveal generalizable principles applicable to vesicle-mediated communication across biological systems.

Materials and methods

Bacterial strains and growth conditions

SP15 is an ExPEC strain isolated from a neonatal meningitis case [17]. SP15, SP15*Δhlyf* HlyF^{wt} and SP15*Δhly*F HlyF^{mut} were previously described in [11]. BL21(DE3) expressing wild-type and mutated HlyF were obtained following transformation with respectively, plasmids pAGO-15 and pAGO-16 previously described in [9]. BL21(DE3) strains were further transformed with pUC19 plasmid for TEM-1 ß-lactamase expression (Addgene). ECC166 is an uropathogenic *E. coli* strain (UPEC) isolated from woman with pyelonephritis. ECC166 and ECC166 Δ*hlyF* strains described in [12] were further transformed with pUC19 plasmid. *P. aeruginosa* PAK *ΔcprA* and PAK *ΔcprA* complemented with CprA strains were previously described in [9]. PAK strains were further transformed with pJN-TEM plasmid in which the *tem-1* gene from pUC19 was inserted into the EcoRI-XbaI sites of pJN105 plasmid (Addgene) under the control of AraBAD promoter. For OMV production, bacteria were grown at 37°C under vigorous shaking (240rpm) for 8h in M63 medium supplemented with casamino-acid and appropriate antibiotic and inoculated with 1/100 of overnight culture. For PAK strains, 1% rhamnose and 1% arabinose were added after 3h of culture for CprA and TEM-1 induction respectively.

Purification of bacterial OMVs

After 8h of culture the bacterial suspension was centrifuged at 6500g for 10min at 4°C. The supernatant was filtered (pore size 0.45 µm; Merck-Millipore) to obtain bacterial-free supernatant. The filtered supernatant was ultrafiltered and concentrated using tangential concentrator and PES membrane cassette (pore size 100kDa; Sartorius) and then ultracentrifuged at 150,000g for 2h at 4°C. After removing the supernatant, pelleted OMV were resuspended in sterile PBS and stored at 4°C. To visualize the concentration of OMVs and

the purity of the preparation, negative staining transmission electron microscopy (TEM) was performed according to standard procedures. The concentration of OMVs in the suspension correlates with protein concentration evaluated by BCA protein assay (Bio-Rad, RC DCTM Protein Assay kit II). OMV diameter was calculated by dynamic light scattering using Zetasizer Nano instrument (Malvern). It should be noted that DLS enables accurate measurement of vesicle sizes below the 50 nm detection limit of NTA (Nano Tracking Analyzis) technology for organic/biologic sample [18, 19]. When indicated, pronase treatment was performed by incubating OMV (125µg/mL) with pronase (2mg/mL) for 90 min at 37°C. Following digestion, samples were supplemented with cOmplete protease inhibitor (Roche) and 1 mM phenylmethylsulfonyl fluoride (PMSF), then ultracentrifuged and resuspended in PBS at initial volume.

Eukaryotic cell culture

HeLa cells (ATCC, HeLa CCL2) were cultured in DMEM with Glutamax (Life Technology) supplemented with 10% fetal bovine serum (FBS) and non-essentials amino-acids (Life Technology). One day before the experiment, HeLa cells were seeded in 96-wells plate at a density of 10^4 cells per well in 100µL of DMEM supplemented with 10% FBS. One week before treatment, bone marrow-derived macrophages (BMDM) were prepared from fresh bone marrow isolated from C57BL/6 mice at a density of 2×10^5 cells per well. Bone marrow cells were allowed to differentiate in macrophages by incubation for 7 days in DMEM supplemented with 10% FBS, 25ng/ml CSF1/M-CSF (Immunotools), 10mM HEPES, pH 7.2 and nonessential amino acids (Life Technology).

CCF4-AM assays

Twenty µL of 6X loading solution with CCF4-AM (LiveBLAzer FRET-B/G loading kit; Life technologies) supplemented with 2.5mM of probenicid were added to 100µL of cell culture in p96-well plate seeded at day-1 and further incubated at room temperature for 2h. Cells were rinsed 3 times with 100µl of HBSS and incubated with indicated concentration of OMVs in OptiMEM medium with probenicid. When indicated, Dynasore (80µM), chloroquine (100µM) or bafilomycin (100nM) were added together with OMVs. Background control wells without CCF4, with and without inhibitors were performed. Each condition was done in triplicate. Plate reading was performed with Tecan Infinite 200 Pro (Tecan) at 37°C, every 15 min during 8h with excitation set at 410nm and detection of emission at 450nm (blue fluorescence) and

520nm (green fluorescence). CCF4-AM cleavage was calculated by the ratio of the net blue fluorescence (- background) divided by the net green fluorescence.

Immunoblotting

Detection of OmpA and ß-lactamase were performed with 2 µg of purified OMVs preparation per lane, separated by SDS-PAGE (Invitrogen) and transferred to PVDF membranes (Invitrogen). The membranes were blocked in 5% non-fat dry milk in TBS 0.1% Tween® 20 and probed with rabbit anti *E. coli* OmpA antibody (Antibody Research Corporation) and mouse anti-beta lactamase antibody [8A5.A10] (Abcam). After incubation with goat anti-rabbit and goat anti-mouse HRP-conjugated secondary antibodies (Bethyl Laboratories), proteins were visualized using chemiluminescent peroxidase substrate detection reagents (Sigma), and acquired by the ChemiDoc XRS+ System (Bio-Rad). Protein quantification was performed by densitometric analyses of immunoblots using the ImageJ software.

Nitrocefin hydrolysis assay

Ten µL of OMVs at 50ng/mL were transferred into a 96-well microplate on ice with 40µL of PBS and 50µL of nitrocefin solution (Euromedex, TO-N005) at 10mg/mL. Each condition was done in triplicate. Absorbance at 486 nm was measured immediately using Infinite 200 Pro plate reader (Tecan) and subsequently every 5 min for 2h.

Lipid extraction

For lipid extraction, we used a Folch-like extraction method [20]. Briefly, bacteria were grown under the same conditions as for OMV production (see OMV production above). After 8 hours of culture at 37°C with agitation at 240 rpm, the cultures were centrifuged at 6000 × g for 10 minutes to pellet the bacteria and remove the supernatant. The bacterial pellet was then resuspended in a 2:1 $CHCl_3$/MeOH solution and agitated for 1 hour at 40 rpm in a rotary shaker. Samples were then centrifugated for 10 min à 1 000 rpm. The supernatants were then washed with water and agitated for 15 min at 40 rpm in a rotary shaker. Samples were then centrifugated for 10 min at 1 000 rpm and the organic phases were recovered and evaporated under N_2. Dry lipids pellets were then resuspended in DMEM 1X without phenol red (21063 Gibco). Lipids concentration were quantified with a sulfo-phospho-vanillin reaction as described in Izard *et al. [21]* with Triolein as reference (44896-U Sigma Aldrich).

Liposomes preparation

Liposomes were generated from mix of lipids derived from HlyF-expressing bacteria (extracted as described above) and a commercial fluorescent lipid, namely 1-palmitoyl-2-{12-[(7-nitro-2-1,3-benzoxadiazol-4-yl)amino]dodecanoyl}-sn-glycero-3-phosphoethanolamine (NBD-PE, 810154P-1MG Avanti), adapted from Kehl *et al. [22]*. Before extrusion, lipidic mixes of 1 mg were prepared with 0.5 mg of lipids from HlyF-expressing bacteria and 0.5 mg of 16:0-12:0 NBD PE (16) resuspended in chloroform/methanol (2/1, v/v). For liposomes-control, a lipidic mix of 1 mg was prepared with 0.5mg of lipids from $HlyF^{mut}$-expressing bacteria and 0.5mg of commercial 16:0-12:0 NBD PE. Lipidic mixes were then evaporated under N_2. Dry lipids pellets were resuspended in DMEM without phenol red (21063 Gibco). Liposomes were then generated by extrusion, according to the manufacturer's instruction about the Avanti Mini Extruder Extrusion Technique (610000-1EA Avanti Polar Lipids Inc.). Lipids mixes were extruded using 200 nm (610006-1EA Avanti) then 100 nm membranes (610005-1EA Avanti) and stored at 4°C. Images were acquired using a Zeiss LSM 710 confocal microscope. Images were subsequently processed using the ImageJ software package.

Fluorescence microscopy

OMVs were labelled with 1% (v:v) DiI (Invitrogen, V22885) for 30 min at 37 °C. HeLa cells were seeded at a density of 5×10^5 cells per well in 1mL of DMEM supplemented with 10% FBS into 12-well plates with slides in the bottom of the wells the day before the experiment. The day of the experiment, cells were treated with 10µg/mL of OMV for the indicated time. When indicated, CtxB-FITC (Sigma, C1655) was added directly in the medium of cell culture at a final concentration of 1µg/mL at the same time as OMV. At the end of the experiment the cells were fixed with 4% PFA for 12 min at RT. After being washed 3 times with PBS the slides were mounted with Fluoroshield (sigma F6182). Images were acquired using a Zeiss LSM 710 confocal microscope. Images were subsequently processed using the ImageJ software package.

Statistical analyses

Statistical analyses were performed on at least 3 independent experiments with the unpaired t-test using the Prism software package (GraphPad Software). Differences were considered significant for the following P-values: *P<0.05; **P<0.01; ***P<0.001; ****P<0.0001.

Figure legends:

Figure 1. Method of measurement of B-lactamase in host cells.

(A) Schematic representation of OMV loaded with ß-lactamase: *E. coli* BL21(DE3) co-transformed with plasmids encoding TEM-1 β-lactamase and either wild-type (*WT*) or mutant (*mut*) *hlyF* produce OMVs containing β-lactamase (magenta) and OmpA (pink barrel) (Biorender ?); (B) Western blot detection of OmpA and TEM-1 β-lactamase from 0.5µg of purified OMVs from BL21 strains expressing wild type ($HlyF^{wt}$) or inactive mutated ($HlyF^{mut}$) HlyF; (C) Representative kinetic assay of nitrocefin hydrolysis measured by O.D. at 486nm over time upon incubation with indicated OMVs (OMVs control correspond to OMVs produced in absence of pUC encoding ß-lactamase) at the same concentration (see also supplementary figure 1A)

Figure 2. HlyF promotes accumulation of TEM-1 β-lactamase in eukaryotic cells.

(A) Principle of CCF4-AM assay: intact CCF4 emits green fluorescence, whereas cleavage by β-lactamase delivered through internalized OMVs results in blue fluorescence due to FRET loss; (B) Time course of blue/green fluorescence ratios in HeLa cells treated with the 10µg/mL of OMVs from BL21(DE3) expressing wild type ($HlyF^{wt}$) or mutated HlyF ($HlyF^{mut}$). Data are representative of triplicate experiments; error bars denote standard error of the mean; (C) Quantification of intracellular TEM-1 β-lactamase activity expressed as the area under the curve (AUC) from panel A, calculated from four independent experiments with 10µg/mL OMVs. Data are mean ± SEM; statistical significance assessed by one-way ANOVA with Bonferroni correction (*$p < 0.05$, **$p < 0.01$, ***$p < 0.001$).

(C) Slopes of blue/green fluorescence curves from panel D determined by linear regression.

(D) Time course of blue/green fluorescence ratio in mouse bone marrow-derived macrophages treated with 20µg/mL of OMVs from BL21(DE3) expressing wild type ($HlyF^{wt}$) or mutated HlyF ($HlyF^{mut}$). Data are representative of triplicate experiments; error bars denote standard error of the mean.

Figure 3. Pharmacological inhibition of OMVs produced by BL21(DE3) expressing wild-type or inactive HlyF. HeLa cells were treated with 10 µg/mL OMVs and intracellular β-lactamase activity quantified as AUC.

(A–C) AUC values for cells incubated with HlyF^{wt} or HlyF^{mut} OMVs in the presence of DMSO (white bars) or pharmacological inhibitors (grey bars): (A) chloroquine (CQ), (B) bafilomycin (Baf), and (C) dynasore (Dyn); (D) AUC values from three independent experiments using HlyF^{wt} OMVs (2µg/mL) or HlyF^{mut} OMVs (5µg/mL) in the presence of dynasore or DMSO. Data are expressed as percentage relative to the HlyF^{wt} + DMSO condition. Error bars denote SEM. Statistical analysis by one-way ANOVA with Bonferroni correction; ns, not significant; ****$p < 0.01$; ****$p < 0.001$.

Figure 4. HlyF^{wt} OMVs are internalized in host cells by direct fusion to plasma membrane.

(A) Confocal microscopy of HeLa cells treated for 2h with 10 µg/mL DiI-stained HlyF^{wt} or HlyF^{mut} OMVs. Scale bar, 10µm. Images are representative of 3 independent experiments; at least 50 cells were analyzed per condition; (B) Confocal microscopy of HeLa cells treated for 6 h with liposomes derived from either HlyF^{wt} or HlyF^{mut} strains (100µg of lipid/mL). Liposomes were visualized using NBD–phosphatidylethanolamine fluorescence (310nm), while nuclei were counterstained with DAPI. Images are representative of two independent experiments. Scale bar, 10 µm; at least 50 cells were analyzed per condition; (C) Confocal microscopy of HeLa cells treated for 1.5h with 5µg/mL HlyF^{wt} or HlyF^{mut} OMVs. Lipid raft distribution was visualized by cholera toxin B subunit conjugated to FITC (CtxB-FITC, green) and bright-field imaging. Scale bar, 10µm. Images are representative of 5 independent experiments; at least 50 cells were analyzed per condition.

Figure 5. OMVs from clinical pathogenic strains expressing HlyF/CprA promote cargo accumulation in host cells.

AUC values representing total delivery of OMV-associated TEM-1 β-lactamase were calculated from time-course experiments as in Figure 1D.

(A) HeLa cells treated with 10µg/mL OMVs from SP15 Δ*hlyF* strain complemented with wt or mut HlyF.

(B) Cells treated with 10 or 20µg/mL OMVs from ECC166 Δ*hlyF* (black bars) or wt (white bars) strains.

(C) Cells treated with 10, 20, or 30µg/mL OMVs from *P. aeruginosa* PAK Δ*cprA* (black bars) or Δ*cprA* complemented with *cprA* (white bars).

Supplementary figure 1. Characterization of OMV produced by BL21(DE3) expressing wild-type or mutated HlyF. (A) Quantification of ß-lactamase activity after 2hr incubation of OMV with nitrocefin from 4 independent experiments; (B) Negative staining transmission electronic microscopy of purified $HlyF^{mut}$ and $HlyF^{wt}$ OMVs (scale bar 100nm); (C) Measurement of OMV diameter by dynamic light scattering; (D) Silver (left) and coomassie blue (right) staining of $HlyF^{mut}$ and $HlyF^{wt}$ OMV proteins runed on SDS-PAGE (−).

Supplementary figure 2. OMV protect ß-lactamase from pronase proteolytic activity : AUC from CCF4 assay with HeLa cells incubated with $HlyF^{mut}$ OMVs or $HlyF^{wt}$ incubated 90 min at 37°C with (+) or whitout (-) pronase (2mg/mL), then treated with PMSF and cOmplete protease inhibitor and ultracentrifuged**.**

Supplementary figure 3. DiI staining of OMVs: Confocal microscopy images of BL21(DE3) $HlyF^{wt}$ or $HlyF^{mut}$ OMVs stained with DiI. Scale bar, 10µm.

References:

1. Schwechheimer C, Kuehn MJ. Outer-membrane vesicles from Gram-negative bacteria: biogenesis and functions. Nature reviews Microbiology. 2015;13(10):605-19. doi: 10.1038/nrmicro3525. PubMed PMID: 26373371.
2. Juodeikis R, Carding SR. Outer Membrane Vesicles: Biogenesis, Functions, and Issues. Microbiol Mol Biol Rev. 2022;86(4):e0003222. Epub 20220926. doi: 10.1128/mmbr.00032-22. PubMed PMID: 36154136; PubMed Central PMCID: PMCPMC9881588.
3. Bielaszewska M, Ruter C, Bauwens A, Greune L, Jarosch KA, Steil D, et al. Host cell interactions of outer membrane vesicle-associated virulence factors of enterohemorrhagic Escherichia coli O157: Intracellular delivery, trafficking and mechanisms of cell injury. PLoS Pathog. 2017;13(2):e1006159. doi: 10.1371/journal.ppat.1006159. PubMed PMID: 28158302; PubMed Central PMCID: PMC5310930.
4. Eren E, Planes R, Bagayoko S, Bordignon PJ, Chaoui K, Hessel A, et al. Irgm2 and Gate-16 cooperatively dampen Gram-negative bacteria-induced caspase-11 response. EMBO Rep. 2020;21(11):e50829. Epub 20201030. doi: 10.15252/embr.202050829. PubMed PMID: 33124769; PubMed Central PMCID: PMCPMC7645206.
5. Park KS, Choi KH, Kim YS, Hong BS, Kim OY, Kim JH, et al. Outer membrane vesicles derived from Escherichia coli induce systemic inflammatory response syndrome. PloS one. 2010;5(6):e11334. doi: 10.1371/journal.pone.0011334. PubMed PMID: 20596524; PubMed Central PMCID: PMC2893157.
6. Pathirana RD, Kaparakis-Liaskos M. Bacterial membrane vesicles: Biogenesis, immune regulation and pathogenesis. Cellular microbiology. 2016. doi: 10.1111/cmi.12658. PubMed PMID: 27564529.
7. Sabatke B, Rossi IV, Sana A, Bonato LB, Ramirez MI. Extracellular vesicles biogenesis and uptake concepts: A comprehensive guide to studying host-pathogen communication. Molecular microbiology. 2024;122(5):613-29. Epub 20230927. doi: 10.1111/mmi.15168. PubMed PMID: 37758682.
8. David L, Taieb F, Penary M, Bordignon PJ, Planes R, Bagayoko S, et al. Outer membrane vesicles produced by pathogenic strains of Escherichia coli block autophagic flux and exacerbate inflammasome activation. Autophagy. 2022;18(12):2913-25. Epub 20220407. doi: 10.1080/15548627.2022.2054040. PubMed PMID: 35311462; PubMed Central PMCID: PMCPMC9673956.
9. Goman A, Ize B, Jeannot K, Pin C, Payros D, Goursat C, et al. Uncovering a new family of conserved virulence factors that promote the production of host-damaging outer membrane vesicles in gram-negative bacteria. J Extracell Vesicles. 2025;14(1):e270032. doi: 10.1002/jev2.70032. PubMed PMID: 39840902.
10. Pin C, David L, Oswald E. Modulation of Autophagy and Cell Death by Bacterial Outer-Membrane Vesicles. Toxins. 2023;15(8). Epub 20230814. doi: 10.3390/toxins15080502. PubMed PMID: 37624259; PubMed Central PMCID: PMCPMC10467092.
11. Murase K, Martin P, Porcheron G, Houle S, Helloin E, Penary M, et al. HlyF Produced by Extraintestinal Pathogenic Escherichia coli Is a Virulence Factor That Regulates Outer Membrane Vesicle Biogenesis. The Journal of infectious diseases. 2016;213(5):856-65. doi: 10.1093/infdis/jiv506. PubMed PMID: 26494774.
12. Chagneau CV, Payros D, Goman A, Goursat C, David L, Okuno M, et al. HlyF, an underestimated virulence factor of uropathogenic Escherichia coli. Clin Microbiol Infect. 2023;29(11):1449 e1- e9. Epub 20230731. doi: 10.1016/j.cmi.2023.07.024. PubMed PMID: 37532127.

13. Kaderabkova N, Bharathwaj M, Furniss RCD, Gonzalez D, Palmer T, Mavridou DAI. The biogenesis of beta-lactamase enzymes. Microbiology (Reading). 2022;168(8). doi: 10.1099/mic.0.001217. PubMed PMID: 35943884; PubMed Central PMCID: PMCPMC10235803.
14. Kunsmann L, Ruter C, Bauwens A, Greune L, Gluder M, Kemper B, et al. Virulence from vesicles: Novel mechanisms of host cell injury by Escherichia coli O104:H4 outbreak strain. Scientific reports. 2015;5:13252. doi: 10.1038/srep13252. PubMed PMID: 26283502; PubMed Central PMCID: PMC4539607.
15. Santos JC, Dick MS, Lagrange B, Degrandi D, Pfeffer K, Yamamoto M, et al. LPS targets host guanylate-binding proteins to the bacterial outer membrane for non-canonical inflammasome activation. EMBO J. 2018;37(6). Epub 20180219. doi: 10.15252/embj.201798089. PubMed PMID: 29459437; PubMed Central PMCID: PMCPMC5852652.
16. Stamenkovic M, Janjetovic K, Paunovic V, Ciric D, Kravic-Stevovic T, Trajkovic V. Comparative analysis of cell death mechanisms induced by lysosomal autophagy inhibitors. Eur J Pharmacol. 2019;859:172540. Epub 20190713. doi: 10.1016/j.ejphar.2019.172540. PubMed PMID: 31310755.
17. Johnson JR, Oswald E, O'Bryan TT, Kuskowski MA, Spanjaard L. Phylogenetic distribution of virulence-associated genes among Escherichia coli isolates associated with neonatal bacterial meningitis in the Netherlands. The Journal of infectious diseases. 2002;185(6):774-84. Epub 20020214. doi: 10.1086/339343. PubMed PMID: 11920295.
18. Arab T, Mallick ER, Huang Y, Dong L, Liao Z, Zhao Z, et al. Characterization of extracellular vesicles and synthetic nanoparticles with four orthogonal single-particle analysis platforms. J Extracell Vesicles. 2021;10(6):e12079. Epub 20210406. doi: 10.1002/jev2.12079. PubMed PMID: 33850608; PubMed Central PMCID: PMCPMC8023330.
19. Bachurski D, Schuldner M, Nguyen PH, Malz A, Reiners KS, Grenzi PC, et al. Extracellular vesicle measurements with nanoparticle tracking analysis - An accuracy and repeatability comparison between NanoSight NS300 and ZetaView. J Extracell Vesicles. 2019;8(1):1596016. Epub 20190401. doi: 10.1080/20013078.2019.1596016. PubMed PMID: 30988894; PubMed Central PMCID: PMCPMC6450530.
20. Folch J, Lees M, Sloane Stanley GH. A simple method for the isolation and purification of total lipides from animal tissues. J Biol Chem. 1957;226(1):497-509. PubMed PMID: 13428781.
21. Izard J, Limberger RJ. Rapid screening method for quantitation of bacterial cell lipids from whole cells. J Microbiol Methods. 2003;55(2):411-8. doi: 10.1016/s0167-7012(03)00193-3. PubMed PMID: 14529962.
22. Kehl A, Kuhn R, Detzner J, Steil D, Muthing J, Karch H, et al. Modeling Native EHEC Outer Membrane Vesicles by Creating Synthetic Surrogates. Microorganisms. 2020;8(5). Epub 20200506. doi: 10.3390/microorganisms8050673. PubMed PMID: 32384757; PubMed Central PMCID: PMCPMC7284840.

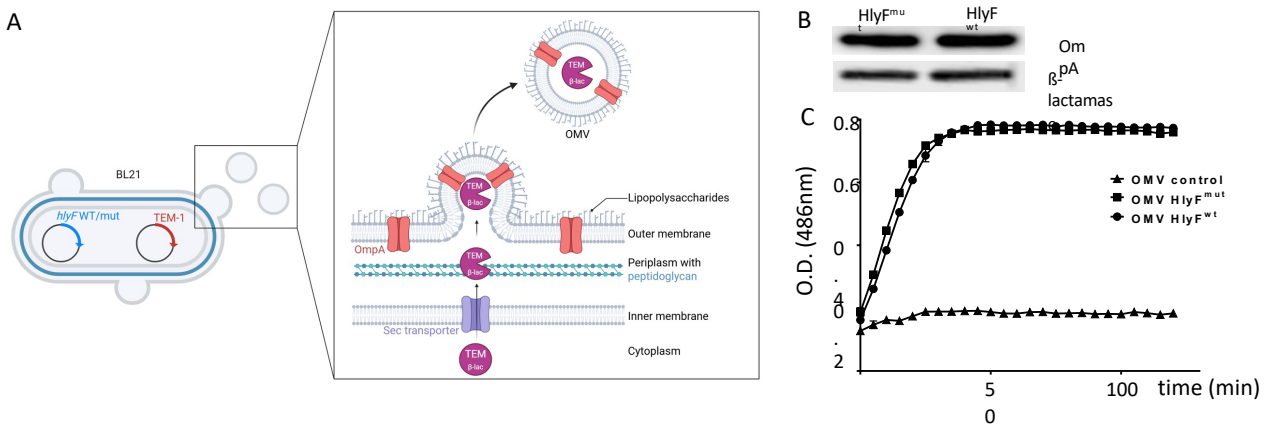
A
BL21
hlyF WT/mut
TEM-1
OMV
TEM
β-lac
Lipopolysaccharides
Outer membrane
OmpA
Periplasm with
peptidoglycan
Inner membrane
Sec transporter
Cytoplasm
B
HlyF
HlyF
Om
pA
ß-
lactamas
C
O.D. (486nm)
0.8
0.6
0.4
0.2
0
5
100
time (min)
OMV control
OMV HlyF
OMV HlyF

Figure 1

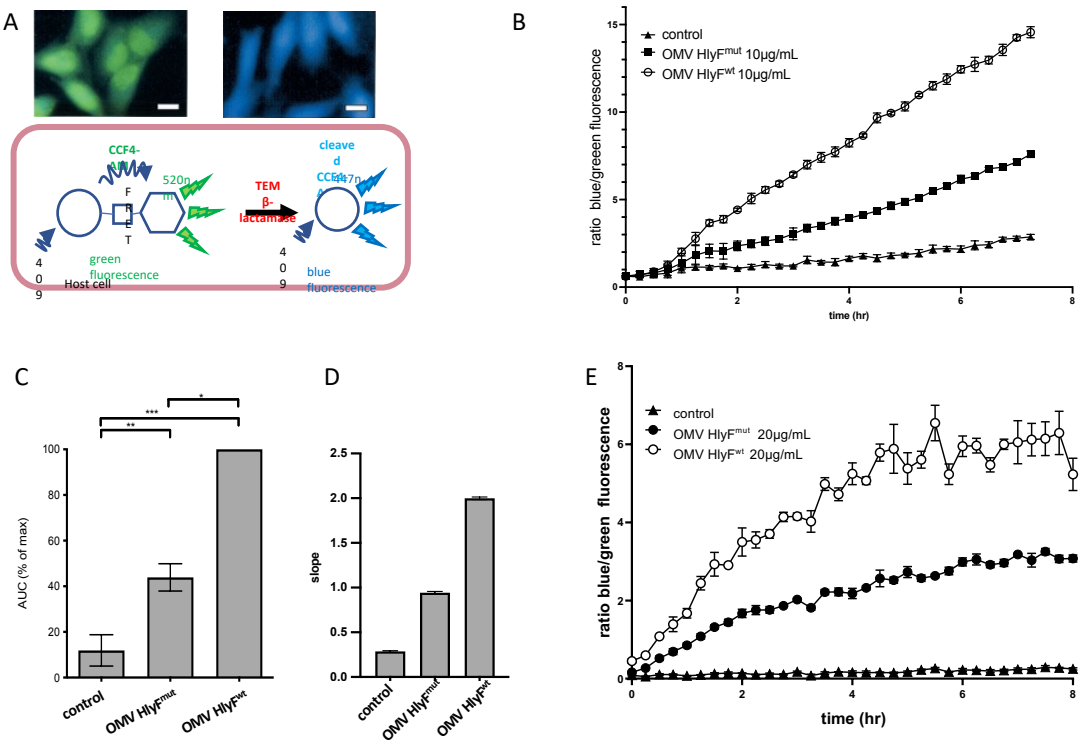
A
CCF4-AM
520nm
F
R
T
TEM β-lactamase
cleaved CCF4
447nm
green fluorescence
Host cell
blue fluorescence
B
control
OMV HlyF^mut 10µg/mL
OMV HlyF^wt 10µg/mL
ratio blue/green fluorescence
time (hr)
C
AUC (% of max)
control
OMV HlyF^mut
OMV HlyF^wt
D
slope
control
OMV HlyF^mut
OMV HlyF^wt
E
control
OMV HlyF^mut 20µg/mL
OMV HlyF^wt 20µg/mL
ratio blue/green fluorescence
time (hr)

Figure 2

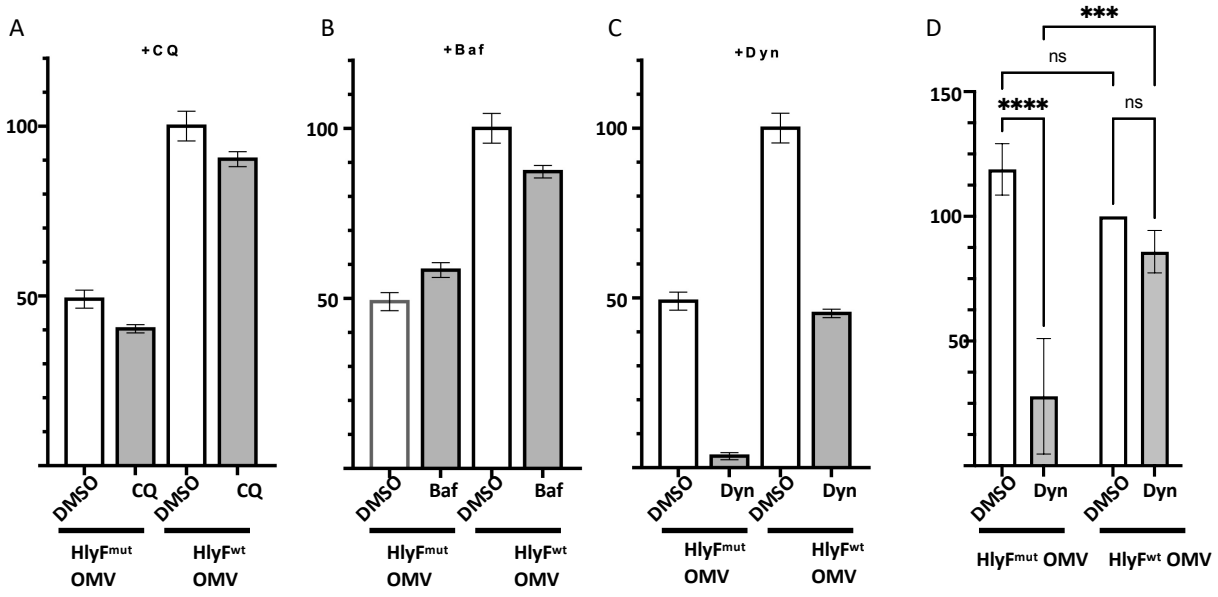
A
+CQ
100
50
DMSO
CQ
DMSO
CQ
HlyFmut OMV
HlyFwt OMV
B
+Baf
100
50
DMSO
Baf
DMSO
Baf
HlyFmut OMV
HlyFwt OMV
C
+Dyn
100
50
DMSO
Dyn
DMSO
Dyn
HlyFmut OMV
HlyFwt OMV
D
***
ns
****
ns
150
100
50
DMSO
Dyn
DMSO
Dyn
HlyFmut OMV
HlyFwt OMV

Figure 3

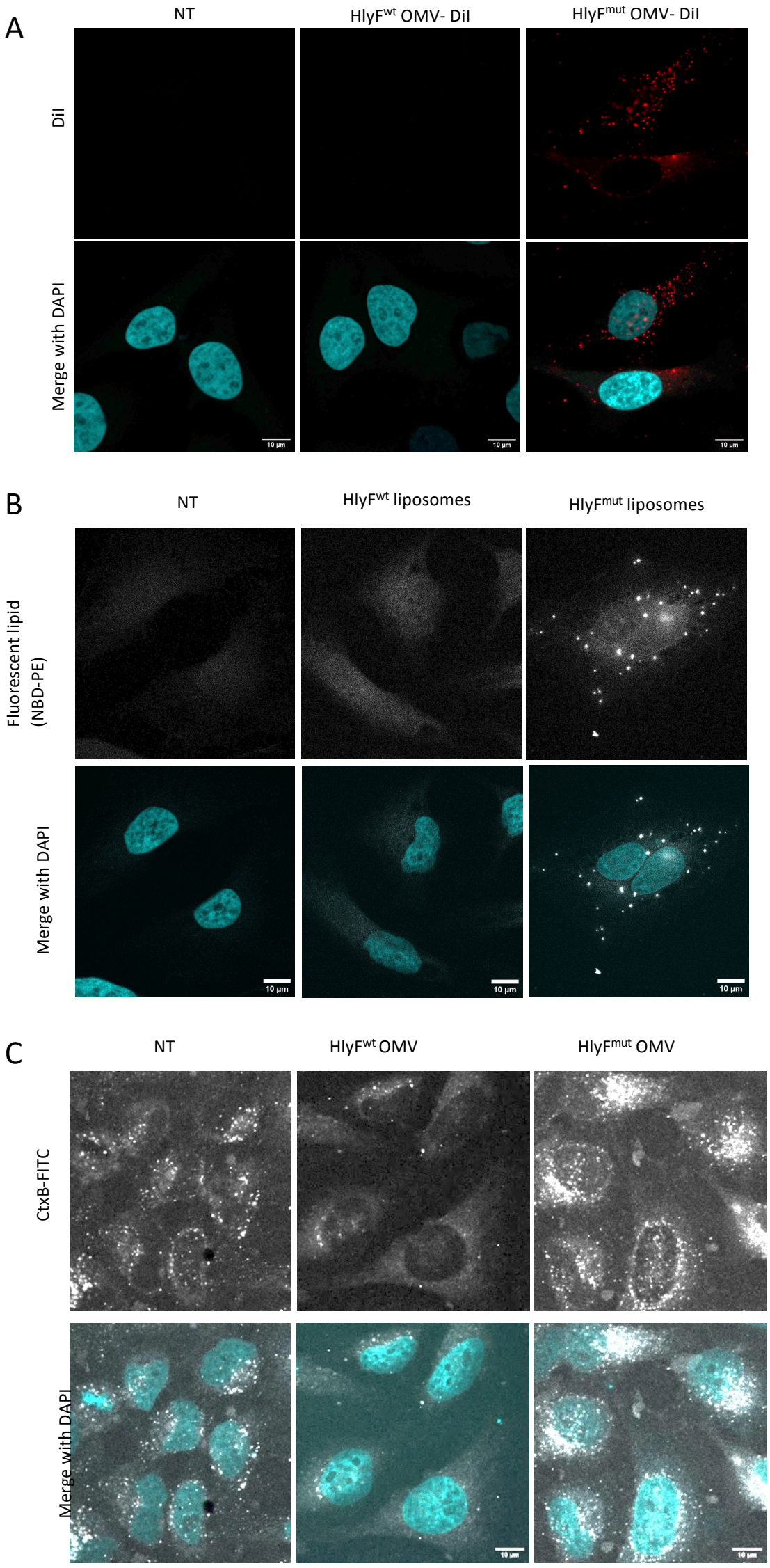
A
NT
HlyF^{wt} OMV- DiI
HlyF^{mut} OMV- DiI
DiI
Merge with DAPI
10 µm
B
NT
HlyF^{wt} liposomes
HlyF^{mut} liposomes
Fluorescent lipid (NBD-PE)
Merge with DAPI
10 µm
C
NT
HlyF^{wt} OMV
HlyF^{mut} OMV
CtxB-FITC
Merge with DAPI

Figure 4

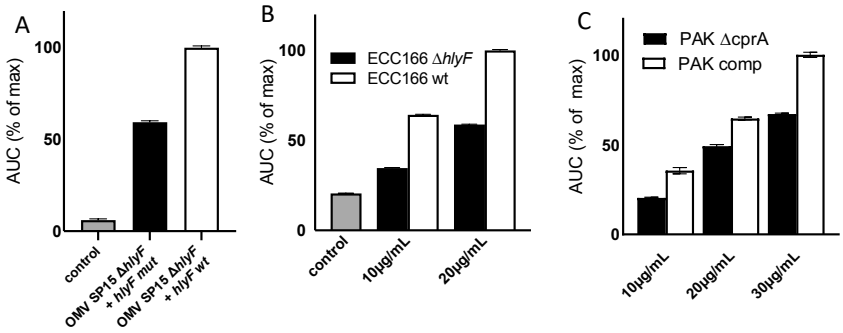
A
AUC (% of max)
100
50
0
control
OMV SP15 ΔhlyF + hlyF mut
OMV SP15 ΔhlyF + hlyF wt
B
AUC (% of max)
100
50
0
ECC166 ΔhlyF
ECC166 wt
control
10µg/mL
20µg/mL
C
AUC (% of max)
100
50
0
PAK ΔcprA
PAK comp
10µg/mL
20µg/mL
30µg/mL

Figure 5

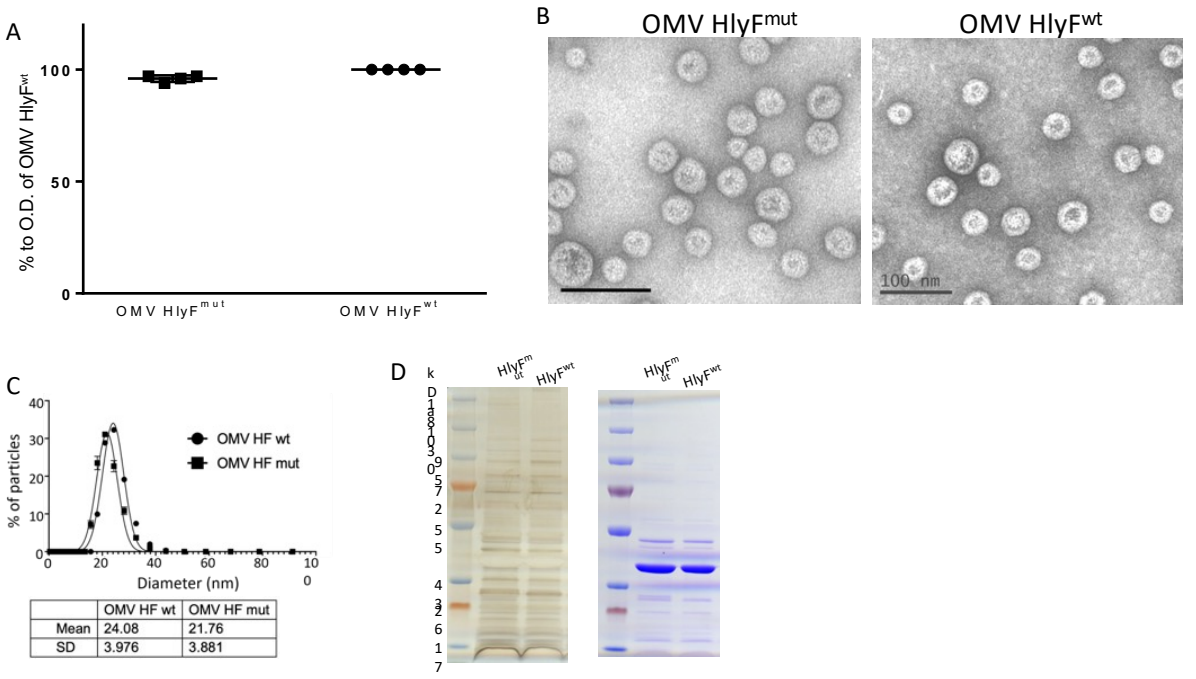

	OMV HF wt	OMV HF mut
Mean	24.08	21.76
SD	3.976	3.881

Supplementary figure 1. Characterization of OMV produced by BL21(DE3) expressing wild-type or mutated HlyF. (A) Quantification of ß-lactamase activity after 2hr incubation of OMV with nitrocefin from 4 independent experiments; (B) Negative staining transmission electronic microscopy of purified $HlyF^{mut}$ and $HlyF^{wt}$ OMVs (scale bar 100nm); (C) Measurement of OMV diameter by dynamic light scattering; (D) Silver (left) and coomassie blue (right) staining of $HlyF^{mut}$ and $HlyF^{wt}$ OMV proteins runed on SDS-PAGE (–)

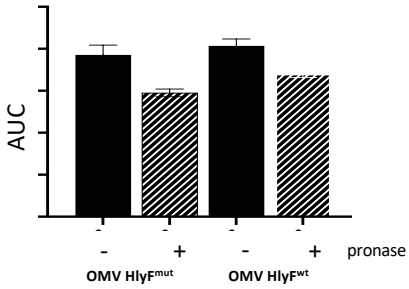

Supplementary figure 2. OMV protect ß-lactamase from pronase proteolytic activity : AUC from CCF4 assay with HeLa cells incubated with HlyF^{mut} OMVs (25µg/mL) or HlyF^{wt} (10µg/mL) treated 90 min at 37°C with (+) or whitout (-) pronase (2mg/mL), then treated with PMSF and cOmplete protease inhibitor and ultracentrifuged.

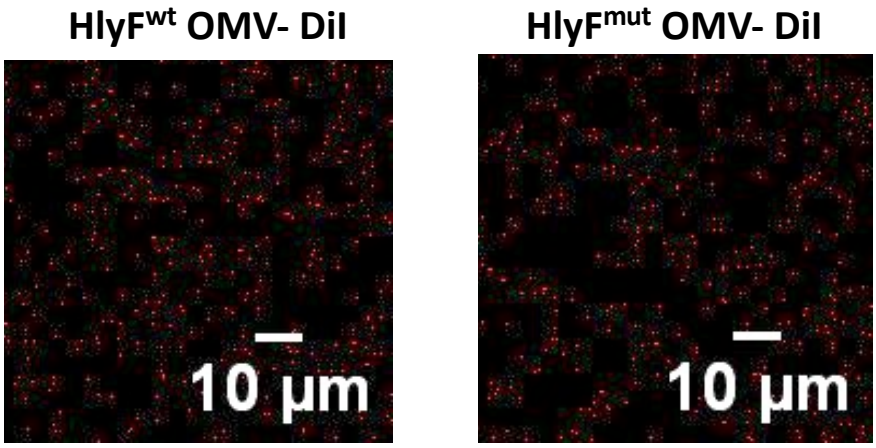

Supplementary figure 3. DiI staining of OMVs: Confocal microscopy images of BL21(DE3) HlyF^{wt} or HlyF^{mut} OMVs stained with DiI. Scale bar, 10µm.